Scientific Research Publishing

Open Journal of Applied Sciences, 2019, 9, 785-798
https://www.scirp.org/journal/ojapps
ISSN Online: 2165-3925
ISSN Print: 2165-3917

Optical and Structural Properties of Chemical Bath Deposited Cadmium Sulphur Selenide ($CdS_{1-x}Se_x$ ($0 \le x \le 1$)) Thin Films

David U. Ngbiche, Isaac Nkrumah, Francis K. Ampong, Mark Paal, Robert K. Nkum, Francis K. Boakye

Department of Physics, Kwame Nkrumah University of Science and Technology, Kumasi, Ghana
Email: inkrumah.sci@knust.edu.gh

How to cite this paper: Ngbiche, D.U., Nkrumah, I., Ampong, F.K., Paal, M., Nkum, R.K. and Boakye, F.K. (2019) Optical and Structural Properties of Chemical Bath Deposited Cadmium Sulphur Selenide ($CdS_{1-x}Se_x$ ($0 \le x \le 1$)) Thin Films. *Open Journal of Applied Sciences*, **9**, 785-798.
https://doi.org/10.4236/ojapps.2019.911064

Received: October 16, 2019
Accepted: November 19, 2019
Published: November 22, 2019

Abstract

The tuneable band gap property of Cadmium-sulphur-selenide ($CdS_{1-x}Se_x$) thin film makes it an appropriate material for a wide range of optoelectronic applications and this has aroused a lot of interest. In this paper, we report the study of Cadmium-sulphur-selenide ($CdS_{1-x}Se_x$) thin films, successfully grown on commercial glass slide substrate by the chemical bath deposition technique. The effect of selenium content (x value) on the structural, and some optical properties have been studied. The bath solution contained cadmium acetate dehydrate [$Cd(CH_3COO)_2{\cdot}2H_2O$], sodium selenosulphate [Na_2SeSO_3] and thiourea [$CS(NH_2)_2$] were used as the sources of Cd^{2+}, Se^{2-} and S^{2+}, respectively. Tartaric acid ($C_4H_6O_6$) was used as a complexing agent. The pH of the solution was adjusted to 12 by drop-wise addition of ammonia. The bath temperature was kept at 90˚C for a deposition time of 1 hour. Post deposition annealing processes of the thin films were performed in a furnace at a temperature of 400˚C for two hours. Both as-deposited and annealed films were characterised by Powder X-Ray Diffraction, Scanning Electron Microscopy, UV-Visible Optical Absorption Spectroscopy and Energy Dispersive X-Ray Analysis. Optical absorption data analysis indicates that direct allowed transitions occur in the films. The band gap of the as-deposited $CdS_{1-x}Se_x$ decreased linearly from 2.34 eV to 1.48 eV, with increasing selenium content, and in the annealed samples, decreased from 1.84 eV to 1.36 eV. X-ray diffraction measurements revealed, that pure CdS, and CdSe had mixed hexagonal and cubic phases. All the remaining ternary compounds were composed of cubic CdS and hexagonal CdSe phases. The annealed samples showed well defined and more intense peaks, suggesting an improvement in crystallinity. The average grain size increased slightly with increasing selenium content. SEM micrographs showed that the films were compact with a smooth texture and good coverage across the entire area of the substrate.

Keywords

Chemical Bath Deposition, Characterization, Cadmium Sulfur Selenide, Thin Films

1. Introduction

Extensive studies have been carried out on CdS and CdSe semiconducting compounds, either as thin films or nanoparticles. This is due to the interesting properties they exhibit such as, high absorption coefficients in the visible and infrared part of the electromagnetic spectrum, good electrical properties (e.g. carrier mobility and lifetime) and the possibility of obtaining adjustable n- or p-type conductivity by doping [1]. Both compounds have direct band gaps with values suitable for photovoltaic applications. In addition, the formation of a homogeneous solid solution over the entire compositional range ($0 \le x \le 1$), by the combination of these two compounds allow the production of very interesting ternary $CdS_{1-x}Se_x$ systems [2]. Such mixed compositions are of interest mainly because they allow tuning of the semiconductor properties (most commonly bandgap and, therefore, spectral sensitivity). These are considered very important for a wide range of optoelectronic applications.

There are several techniques available for the fabrication of binary and ternary semiconductor materials in varying sizes. Among these techniques, CBD offers a simple and inexpensive route to deposit semiconductor nanostructures and thin films. CBD is currently one of the fastest growing techniques of materials research since this deposition method is straightforward, inexpensive and yields high quality materials that are interesting for applications in various optical and electronic devices. CBD is becoming an important deposition technique for thin films of compound materials like chalcogenides [3]. Another attractive feature of the CBD process is the ease with which alloys can be generated without the use of any sophisticated instrumentation and process control [4]. Post deposition annealing is also an important technique in thin film fabrication, which can help enhance the properties of the thin film by changing the microstructure and phases.

As a follow up to our earlier publication, Hone *et al*. [5], we reported the chemical bath deposition of CdSe thin films, from baths containing Cadmium acetate as the source of cadmium ions and tartaric acid as a complexing agent. The bath temperature was 80˚C, pH of 10 and a deposition time of ninety minutes. We further explained that, this was the first time cadmium acetate was being used as the source of cadmium ions in combination with tartaric acid as a complexing agent for the deposition of CdSe thin films. In this present work, the deposition parameters reported in Hone *et al*. [5], have been modified to synthesize the ternary $CdS_{1-x}Se_x$ ($0 \le x \le 1$). The optical and structural properties of the as-deposited and annealed films are studied. To the best of our knowledge, this work provides a new synthesis route for the chemical bath deposition of $CdS_{1-x}Se_x$ ($0 \le x \le 1$) thin films.

2. Materials and Methods

The starting chemicals used for the deposition were 0.25 M cadmium acetate dehydrate [Cd $(CH_3COO)_2 \cdot 2H_2O$], as the source of cadmium ions, 0.25 M sodium selenosulphate [Na_2SeSO_3] which provided selenium ions, 0.25 M thiourea [$CS(NH_2)_2$] as the source of sulphur ions and 0.1 M tartaric acid [$(CHOH \cdot COOH)_2$] as a complexing agent. Ammonia (NH_3) was used to adjust the pH of the aqueous solutions.

The 0.25 M sodium selenosulphate (Na_2SeSO_3) was prepared by dissolving 3.088 g of Na_2SO_3 in distilled water and transferring into a 100 ml volumetric flask. Distilled water was then added to make up the final volume of 100 ml. The solution was then shaken thoroughly to have a uniform sodium sulphite solution. This was then heated to a temperature of 80˚C with continuous stirring. 1.954 g of elemental selenium powder (99.9% pure) was added to the solution at 80˚C. The mixture was then heated for 8 hours while stirring continuously to obtain Na_2SeSO_3. The solution was left in the container to cool down and then sieved to obtain a clear solution of Na_2SeSO_3. All the chemicals used were of analytical grade.

The mixture for the bath was prepared by dissolving the appropriate amount of cadmium acetate and tartaric acid in a 100 ml beaker. The pH of the solution was adjusted to 12 by addition of ammonia. 10 ml of sodium selenosulphate [Na_2SeSO_3] and some distilled water were added to obtain a final volume of 65 ml. Pre-treated glass slides were immersed vertically in the reaction vessel which was then placed in a water bath maintained at a temperature of 90˚C and continuously stirred for deposition. After 1 hour the slides with the deposited films were removed, washed with distilled water and dried under ambient conditions before film characterization. Films of different compositions were deposited by mixing the prepared solutions of cadmium acetate, thiourea and sodium selenosulphate in the required stoichiometric ratio of $1:(1-x):x$. The composition parameter "x" was obtained by adjusting the volume concentrations of S^{2-} and Se^{2-} ions sources in the stock solution. Post deposition annealing process of the thin films were performed in a closed furnace at a temperature of 400˚C for two hours. The as-deposited cadmium sulphide appeared yellowish to the naked eye and changed to purple with the addition of selenium. After annealing, cadmium sulphide appeared orange and the selenium rich films changed to a darker brown colour.

Structural characterization of the as-deposited and annealed thin films were carried out by a Panalytical X'Pert PRO X-ray diffractometer operating at 45 kV and 40 mA with Cu K_α monochromatic radiation (λ = 0.15406 nm). Optical properties were studied by measuring the absorbance of the thin films at room temperature using a Shimadzu UVmini-1240 UV-Vis single beam spectrophotometer. SEM images and EDX analyses were obtained using a Phenom instrument with nominal electron beam voltage of 15 kV respectively.

3. Results and Discussion

3.1. Optical Properties Studies

Generally, the optical properties of the semiconductors, especially the absorption spectra and optical band gaps, are intensively affected by their band structure, which is basically dominated by the microstructure [6]. The absorbance spectra of the $CdS_{1-x}Se_x$ ($0 \le x \le 1$) thin films are shown in **Figure 1**. The spectra were taken within the wavelength range of 200 to 1100 nm at room temperature.

From **Figure 1**, the samples exhibit a strong and broad absorption edge in the range of 450 to 700 nm. It can also be observed from the optical spectra that there is a shift in the fundamental absorption edge towards longer wavelengths (red shift) with increasing selenium content. This suggests a decrease in band gap which may be attributed to an increase in grain size as sulfur is substituted by selenium [7]. It can also be observed that the absorbance of CdS is higher than CdSe. This is because CdS deposited under these conditions resulted in thicker films. A similar observation was also reported by Hodes [3].

The absorbance spectra of the annealed films also follow a similar pattern.

3.2. The Optical Band Gap

The energy band gap and transition type was determined using the relationship given by Stern [8];

$$A = \frac{\left[K\left(h\upsilon - E_g\right)\right]^{n/2}}{h\upsilon} \tag{1}$$

where v is the frequency, h is the Planck's constant, K is a constant while n carries the value of either 1 for direct transition or 4 for indirect transition. Since CdS and CdSe have direct transitions, it follows that their mixed compositions are also direct transitions, hence, n = 1. **Figure 2** shows $(Ahv)^2$ as a function of

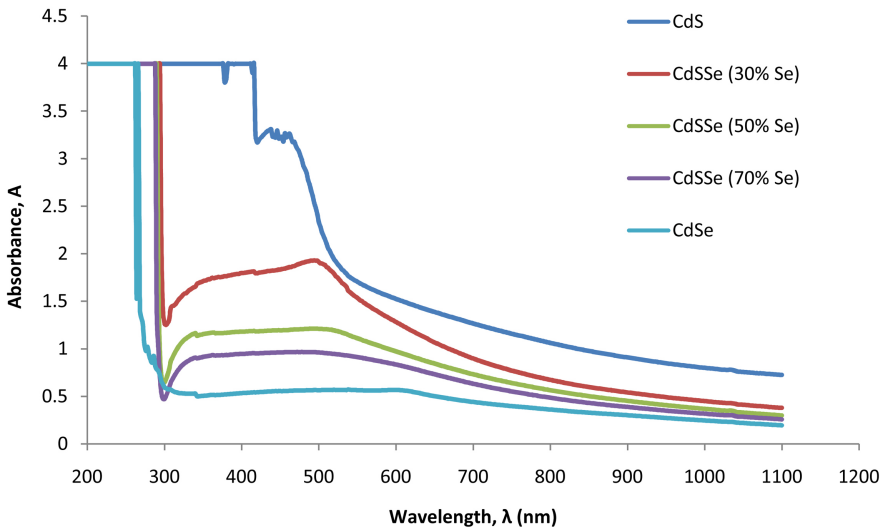

Figure 1. Optical absorbance versus wavelength of the as-deposited $CdS_{1-x}Se_x$ ($0 \le x \le 1$) thin films with increasing Se concentration.

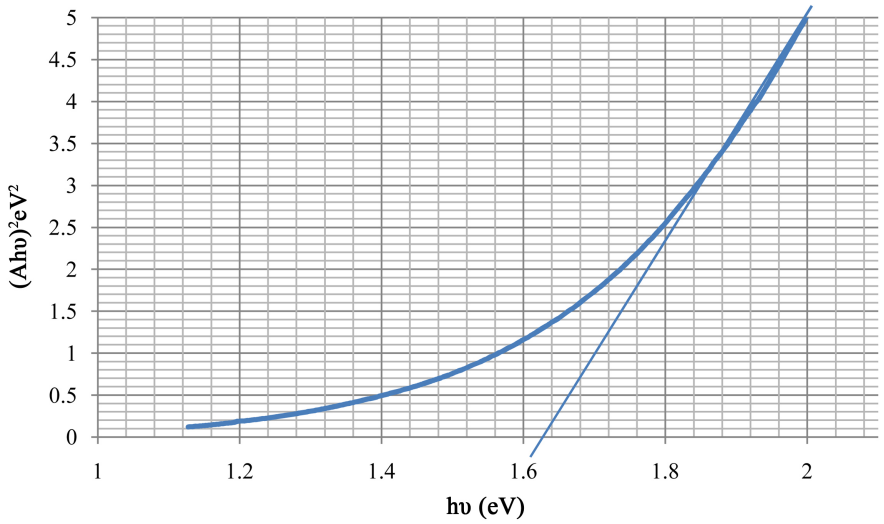

Figure 2. $(Ah\nu)^2$ plotted as a function of $(h\nu)$ based on measurement data from the $CdS_{0.2}Se_{0.8}$ thin film.

$h\nu$. The energy band gap is obtained by plotting a line of best fit to the linear portion of the graph at high $h\nu$ and extrapolating it to the point where it intersects the $h\nu$ axis as shown in **Figure 2**. The linear nature of the graph at high $h\nu$ indicates the presence of a direct transition. From **Figure 2**, the band gap of $CdS_{0.2}Se_{0.8}$ thin film is found to be 1.62 eV.

A graph of the variation of optical band gap value with Se mole concentration "x" is shown in **Figure 3**.

From **Figure 3**, the band gap of the as-deposited $CdS_{1-x}Se_x$ decreased from 2.34 eV to 1.48 eV, with increasing selenium content, and in the annealed samples, decreased from 1.84 eV to 1.36 eV. This nearly linear variation in band gap with Se concentration is an indication of the formation of a continuous series of solid solution [5]. Several investigators have offered various explanations for the decrease in band gap after annealing. Ezugwu *et al.* [9] explained that, the temperature dependence parameters that affect the band gap are reorganization of the film, change in the crystallite size of the film and self-oxidation. According to Chikwenze and Nnabuchi [10], reorganization of the films occurs at all annealing temperatures, which may then fill the voids in the films resulting in denser films and lower band gaps. They further explained that as the size of a semiconductor becomes larger, its direct allowed band gap decreases. In this work, the annealed films appeared to be darker as compared to their as-deposited counterparts. This change in colour is a manifestation of a change in grain size. The decrease in band gaps of the annealed films could be attributed to an increase in grain size as a result of smaller grains coalescing to form larger grains during the annealing process. This supports the explanations offered by Ezugwu *et al.* [9] and Chikwenze and Nnabuchi [10]. Semiconductors with an optical band gap within the range of 1 - 1.5 eV are suitable for achieving high energy conversion efficiency (about 30%) when used as an absorber material in solar

cell applications. The optical band gap of $CdS_{1-x}Se_x$ thin films can be controlled in an optimal region of 1 - 1.5 eV for photovoltaic application.

3.3. X-Ray Diffraction Studies

The X-ray diffractograms of CdS, CdSe, $CdS_{0.9}Se_{0.1}$ (as-deposited and annealed), $CdS_{0.6}Se_{0.4}$ $CdS_{0.4}Se_{0.6}$ are presented in **Figures 4-9** respectively. The peaks were matched to standards in the ICDD database. The different assigned peaks are mentioned in the figures.

In **Figure 4**, the spectrum shows several discernible peaks against a noisy background. The presence of several peaks is an indication of the polycrystalline nature of the sample. The pattern of prominent peaks were indexed to the (111)c, (200)c and (311)c of the cubic CdS phase [ref code: ICDD 01-080-0019], some low intensity peaks were indexed to the (102)h, (202)h and (203)h of the hexagonal CdS phase [ICDD: 01-075-1545]. The films had preferred orientation

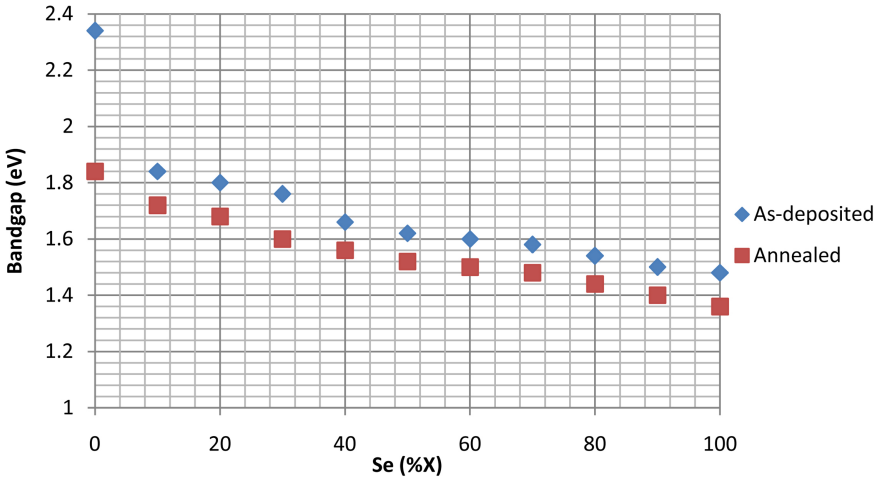

Figure 3. Variation of optical band gap with Se mole concentration "x" for the as-deposited and annealed samples.

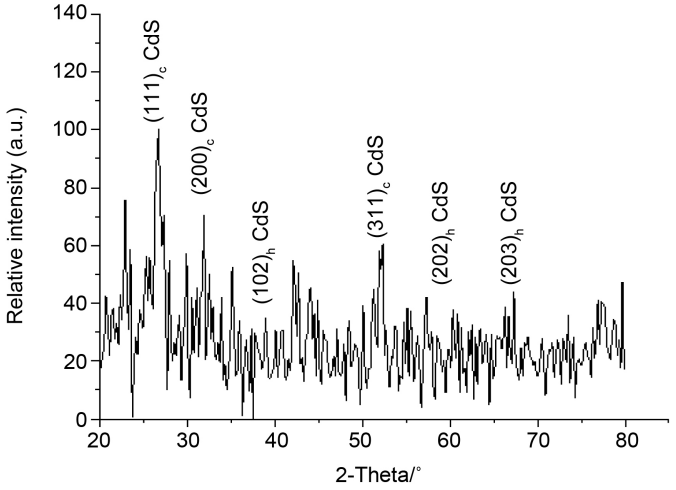

Figure 4. XRD of the as-deposited CdS thin film.

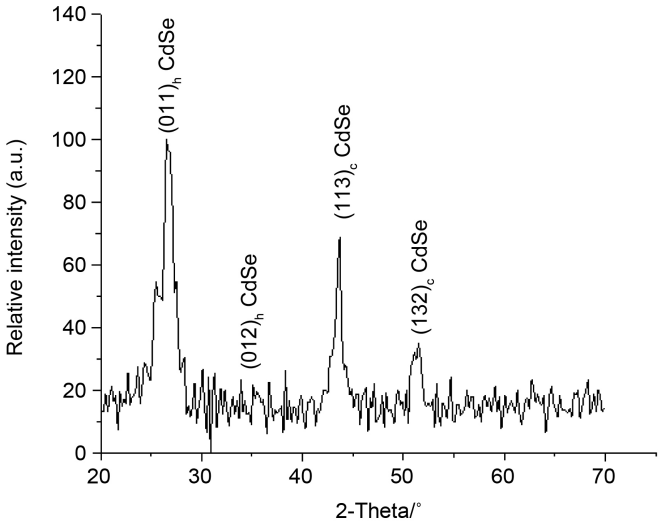

Figure 5. XRD of the pure as-deposited CdSe thin film.

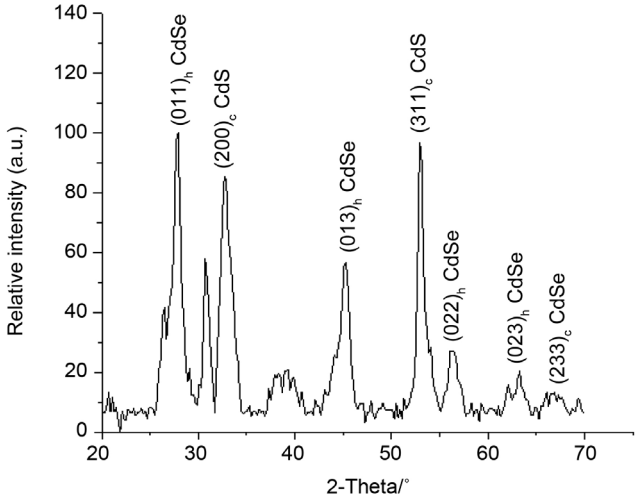

Figure 6. XRD of as-deposited $CdS_{0.9}Se_{0.1}$ thin film.

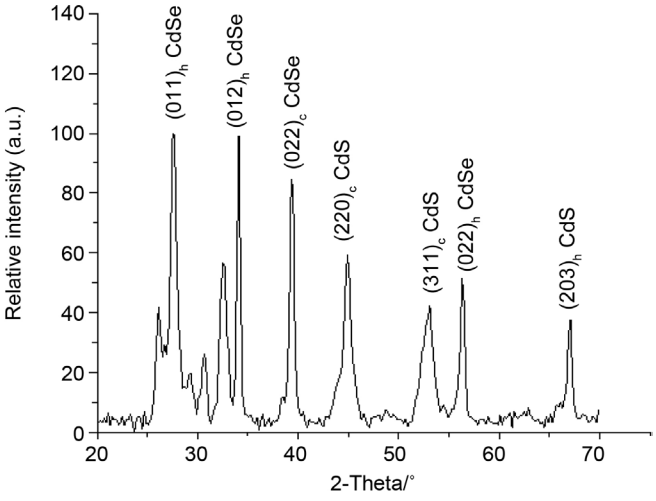

Figure 7. XRD of annealed $CdS_{0.9}Se_{0.1}$ thin film.

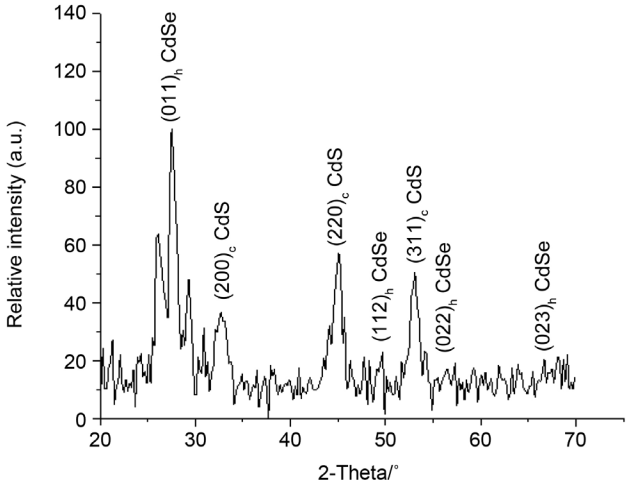

Figure 8. XRD of as-deposited $CdS_{0.6}Se_{0.4}$ thin film.

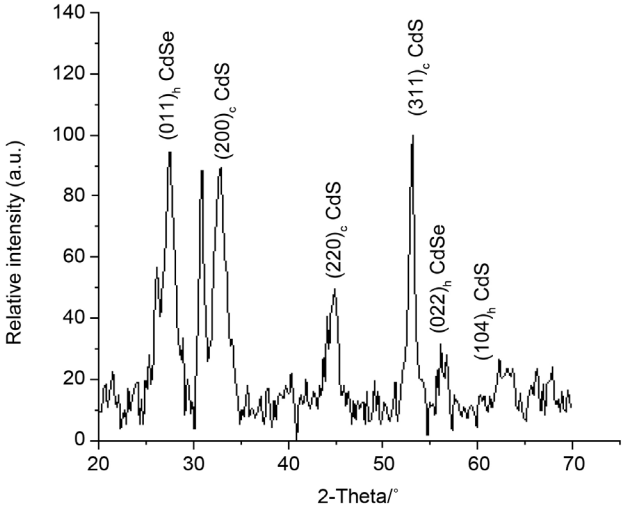

Figure 9. XRD of as-deposited $CdS_{0.4}$-$Se_{0.6}$ thin film.

along the (111)c plane. **Figure 5** shows the diffraction pattern of the pure as-deposited CdSe thin film. The spectrum shows mixed phases of cubic CdSe ((113)c, (132)c [ICDD: 98-062-0416]) and hexagonal CdSe ((011)h, (012)h) with the preferred orientation along the (011) plane of the hexagonal phase of CdSe. This was the first observation of the cubic phase of CdSe in all the samples. The x-ray diffraction pattern of the as-deposited and annealed $CdS_{0.9}Se_{0.1}$ are shown in **Figure 6** and **Figure 7** respectively. The spectrum shows the presence of the cubic CdS and hexagonal CdSe [ICDD: 96-900-8864]. There are no peaks corresponding to the hexagonal CdS phase. The annealed sample showed well defined and more intense peaks, suggesting an improvement in crystallinity. **Figure 8** and **Figure 9** also show the presence of the cubic phase of CdS and the hexagonal phase of CdSe.

A careful analysis of all the XRD patterns reveal a number of interesting features: the binary compounds, CdS and CdSe, as shown in **Figure 4** and **Figure 5**

have mixed hexagonal and cubic phases. Singh and Bhushan [1] have suggested that, the pure CdS thin film might be described as consisting of different atomic layers of CdS in cubic as well as hexagonal phases. A similar explanation can be used for the pure CdSe thin film. Hodes [3] carried out an extensive study on the chemical bath deposition of CdS, and CdSe. The study examined the crystal structure, optical and electrical properties of the thin films, as well as variants of the deposition process. On the crystal structure of CdS, the author reported that the energy difference between the hexagonal (wurtzite) and cubic (zincblende) phases is very small (the former is slightly more stable) hence it is not surprising to observe a mixture of these phases. Such mixed phases were also reported in CdSe thin films deposited from baths containing selenosulphate as the Se source. The author also explained that in view of the lack of a convincing explanation of why one or the other crystal structure is formed, differences in preparation from the standard bath (if any) may be responsible for the crystal modification obtained.

It was also observed that all the $CdS_{1-x}Se_x$ ternary films consisted of cubic CdS and hexagonal CdSe. Typical examples are shown in **Figure 8** and **Figure 9**. Langer *et al*. [11], described a possible structure for this observation. According to the authors, one can consider the solid solutions being composed of mixtures of microcrystalline regions of the pure CdSe and CdS, where each microregion might consist of up to 1000 unit cells of each material, with the lattice constant of CdS stressed by the surrounding CdSe and that of CdSe compressed by its CdS neighbours. This view is supported by calculating the variations in the lattice constant "*a*" of the cubic CdS and lattice constants "*a*" and "*c*" of the hexagonal CdSe with increasing selenium concentration. The following equations were used to calculate the lattice constants

$$a = d\sqrt{h^2 + k^2 + l^2} \tag{2}$$

$$\frac{1}{d^2} = \frac{4}{3}\left[\frac{h^2 + hk + k^2}{a^2}\right] + \frac{l^2}{c^2} \tag{3}$$

The lattice constant of cubic CdS was computed from Equation (2) using data from the (311)c plane, whilst that of the hexagonal CdSe was computed from Equation (3), using data from the (011)h plane. The plots are shown in **Figure 10** and **Figure 11**.

From **Figure 10**, it can be observed that lattice constant of CdS generally increases with Se percentage concentration indicating a pull by the surrounding CdSe leading to expansion. It can also be observed from **Figure 11** that the lattice constant of CdSe also decreases with Se percentage concentration which shows compression by the CdS neighbours. Such a model could explain the uniform shift of absorption edge with variation in composition [11].

A simpler model describing the solid solutions as consisting of a statistical distribution of CdSe and CdS with respect to their overall concentrations was also mentioned by Langer *et al*. [11].

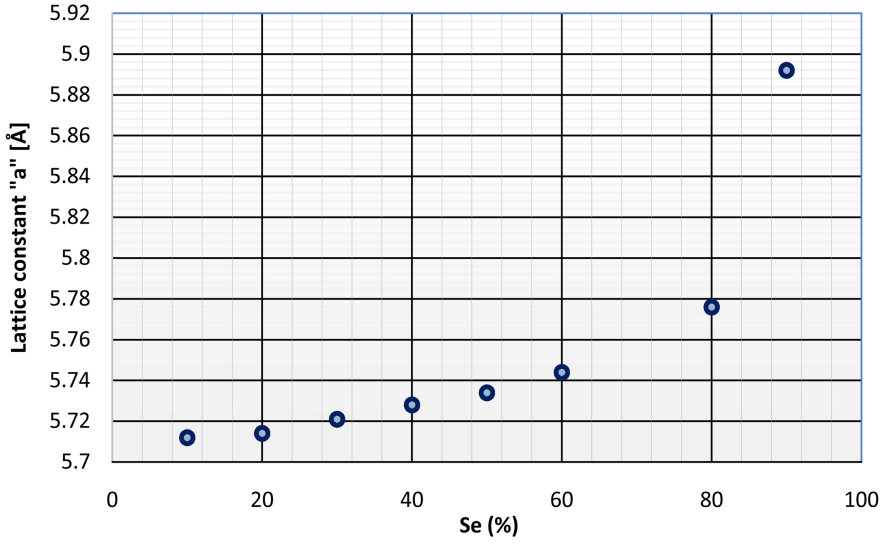

Figure 10. Variation of lattice constant "*a*" of (311)c CdS with Se mole concentration "x" for the as-deposited samples.

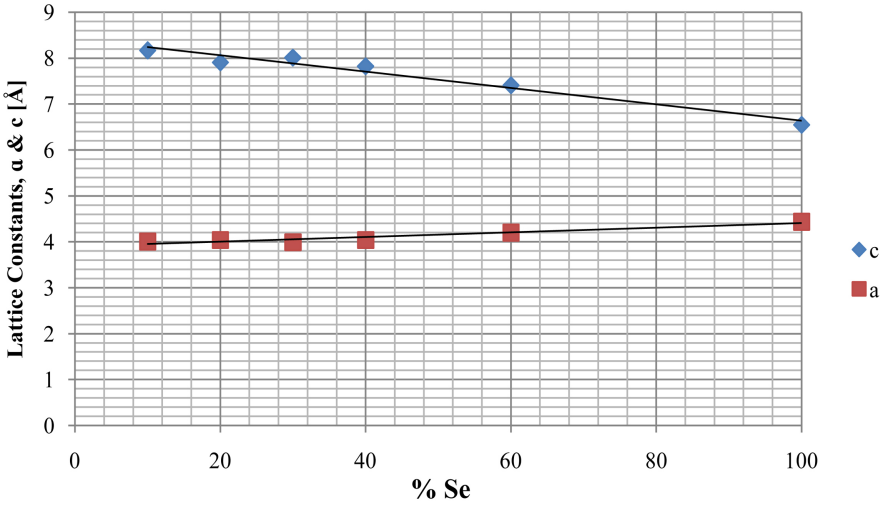

Figure 11. Variation of lattice constants "a" and "c" of (011)h CdSe with Se mole concentration "x" for the as-deposited samples.

Calculation of the average grain size of all the compositions $CdS_{1-x}Se_x$, ($0 \le x \le 1$) was done using the Scherrer [12] formula which is given as:

$$D = \frac{K\lambda}{\beta \cos\theta} \tag{4}$$

where D is the crystallite size, λ is the X-ray wavelength, β full width at half maximum (FWHM) or integral breadth, θ is the Bragg angle and K is a constant [13].

A plot of the variation in crystallite size against selenium composition is shown in **Figure 12**.

From the graph the average grain size increased slightly with the Se content. This supports observations made in the optical analyses that the decrease in energy band gap of the films with increasing Se content can be attributed to an

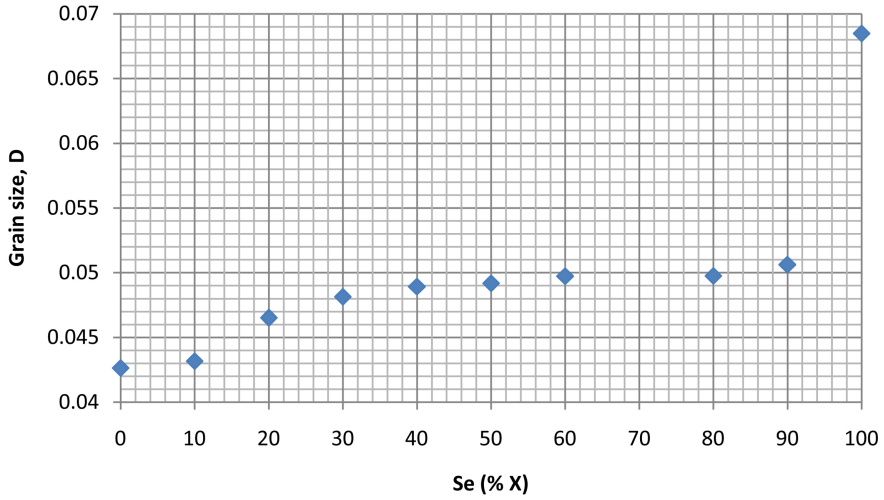

Figure 12. Variation of grain size, D with Se mole concentration "x" for the as-deposited samples.

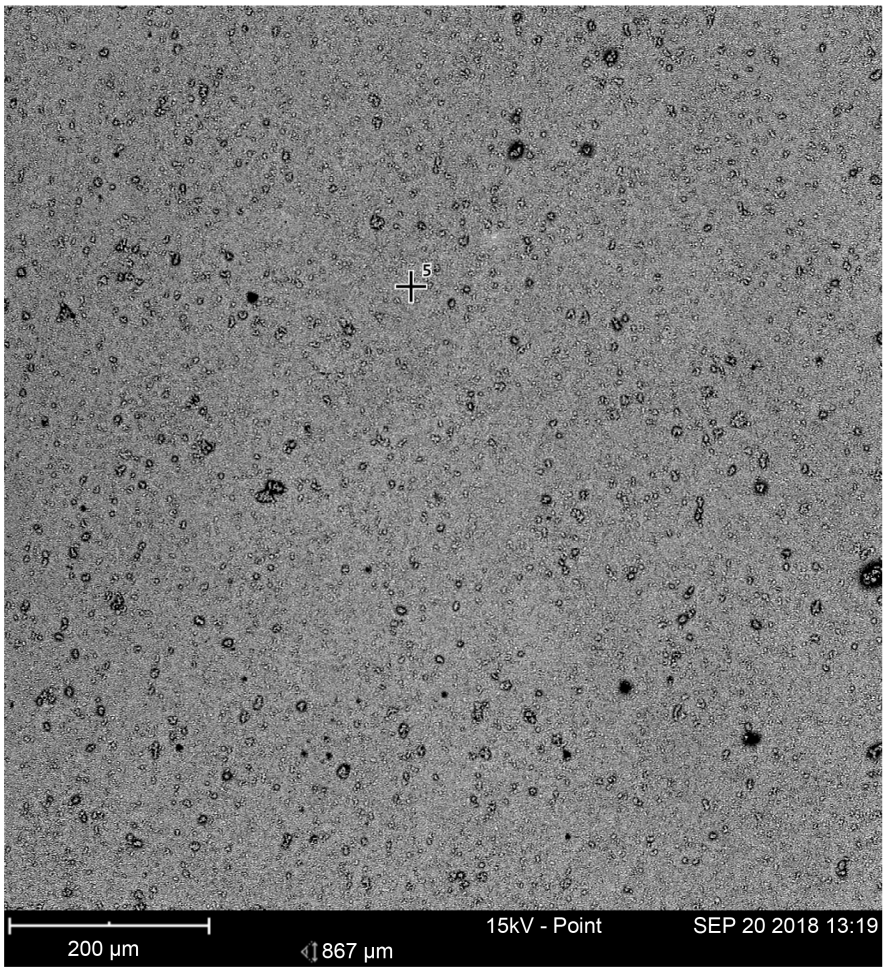

Figure 13. SEM image of $CdS_{0.2}Se_{0.8}$.

increase in grain size. Other structural parameters such as variation in lattice constants, shown in **Figure 10** and **Figure 11**, may also contribute to the observed

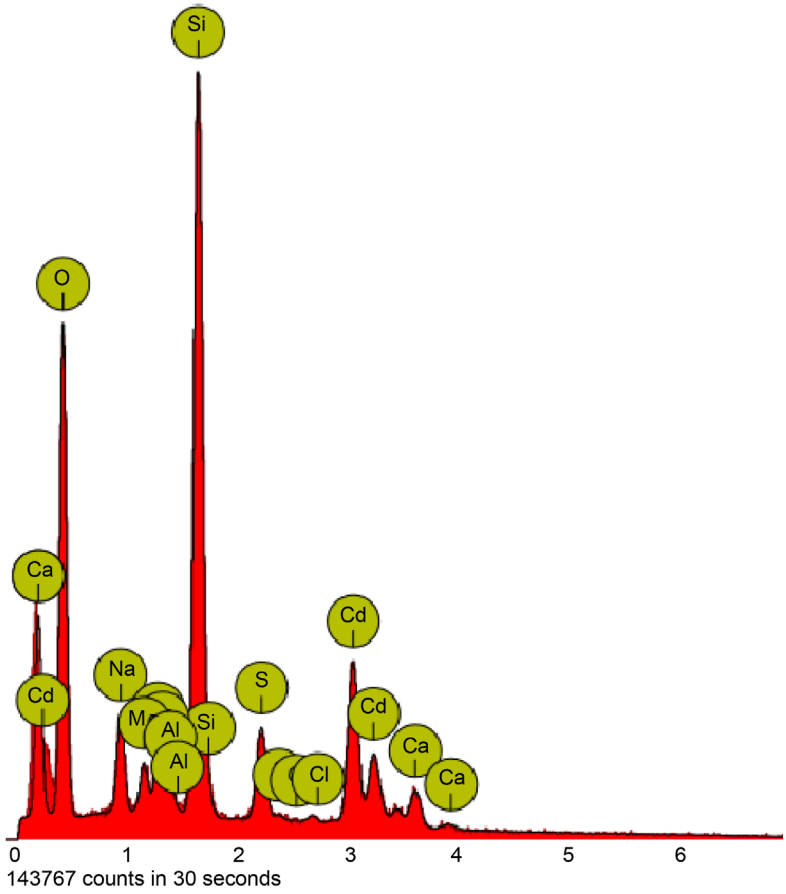

Figure 14. EDAX spectrum of $CdS_{0.2}Se_{0.8}$.

optical behaviour.

Figure 13 is a SEM image of $CdS_{0.2}Se_{0.8}$. The image shows a uniform particle size distribution across the surface of the substrate with no pronounced voids. Film appears compact with a smooth texture and good coverage across the entire area of the substrate. All the films showed a similar morphology.

Figure 14 is the EDAX spectrum of $CdS_{0.2}Se_{0.8}$. The spectrum is consistent with formation of the binary compound on silica glass substrate. The other elements such as Si, Ca, Mg and Al emanate from the glass slide.

4. Conclusion

A new synthesis route has been used to successfully deposit $CdS_{1-x}Se_x$ ($0 \le x \le 1$), thin films by the chemical bath deposition technique. X-ray diffraction measurements revealed, that pure CdS, and CdSe had mixed hexagonal and cubic phases. All the remaining ternary compounds were composed of cubic CdS and hexagonal CdSe phases. There was no phase changes observed in the annealed samples, however, they showed well defined and more intense peaks, suggesting an improvement in crystallinity. The average grain size increased slightly with increasing Selenium content. Structural parameters such as, lattice constants and average grain size varied with increasing selenium content. SEM micrographs

showed that the films were compact with a smooth texture and good coverage across the entire area of the substrate. Optical Absorption Spectroscopy showed that Vergard's law [14] was well established and the optical band gap of the $CdS_{1-x}Se_x$ thin films can be controlled in an optimal region of 1 - 1.5 eV for photovoltaic application. Any future work would include further characterization techniques such as Photoluminescence measurements and further studies on the surface morphology.

Acknowledgements

The authors wish to acknowledge the Department of Physics, and the Department of Earth science, both in the University of Ghana, Legon, for the use of the X-ray diffraction equipment, scanning electron microscope and the energy dispersive X-ray machine.

Conflicts of Interest

The authors declare no conflicts of interest regarding the publication of this paper.

References

[1] Singh, R.S. and Bhushan, S. (2009) Structural and Optical Properties of Chemically Deposited Cd(S-Se):$CdCl_2$, Sm Films. *Bulletin of Materials Science*, **32**, 125-133. https://doi.org/10.1007/s12034-009-0019-7

[2] Murali, K.R. and Venkatachalam, K. (2008) Electrical Properties of Sintered CdS_x Se_{1-x} Films. *Chalcogenide Letters*, **5**, 181-186.

[3] Hodes, G. (2002) Chemical Solution Deposition of Semiconductor Films. Marcel Dekker Inc., New York, 30-40. https://doi.org/10.1201/9780203909096

[4] Barote, M.A., Yadav, A.A. and Masumdar, E.U. (2011) Effect of Deposition Parameters on Growth and Characterization of Chemically Deposited $Cd_{1-x}Pb_xS$ Thin Films. *Chalcogenide Letters*, **8**, 129-138.

[5] Hone, F.G., Ampong, F.K., Abza, T., Nkrumah, I., Nkum, R.K. and Boakye, F. (2015) Synthesis and Characterization of CdSe Nanocrystalline Thin Film by Chemical Bath Deposition Technique. *International Journal of Thin Films Science and Technology*, **4**, 69-74.

[6] Sun, X., Gao, K., Pang, X. and Yang, H. (2016) Interface and Strain Energy Revolution Texture Map to Predict Structure and Optical Properties of Sputtered PbSe Thin Films. *ACS Applied Materials & Interfaces*, **8**, 625-633. https://doi.org/10.1021/acsami.5b09724

[7] Hone, F.G., Ampong, F.K., Nkum, R.K. and Boakye, F. (2017) Band Gap Engineering in Lead Sulphur Selenide ($PbS_{1-x}Se_x$) Thin Films Synthesized by Chemical Bath Deposition Method. *Journal of Materials Science*: *Materials in Electronics*, **28**, 2893-2900. https://doi.org/10.1007/s10854-016-5874-6

[8] Kassim, A., Tan, W.T., Haron, Md.J., Min, H.S., Gwee, S.Y. and Nagalingam, S. (2010) Effects of Deposition Period on the Properties of FeS_2 Thin Films by Chemical Bath Deposition Method. *Thammasat International Journal of Science and Technology*, **15**, 62-69.

[9] Ezugwu, S.C., Ezema, F.I., Osuji, R.U., Asogwa, P.U., Ekwealor, A.B.C. and Ezekoye,

B.A. (2009) Effect of Deposition Time on the Band-Gap and Optical Properties of Chemical Bath Deposited CdNiS Thin Films. *Optoelectronics and Advanced Materials—Rapid Communications*, **3**, 141-144.

[10] Chikwenze, R.A. and Nnabuchi, N.N. (2010) Effect of Deposition Medium on the Optical and Solid State Properties of Chemical Bath Deposited CdSe Thin Films. *Chalcogenide Letters*, **7**, 389-396.

[11] Langer, D.W., Park, Y.S. and Euwema, R.N. (1966) Phonon Coupling in Edge Emission and Photoconductivity of CdSe, CdS and Cd(Se_xS_{1-x}). *Physical Review*, **152**, 788-796. https://doi.org/10.1103/PhysRev.152.788

[12] Sathe, D.J., Chate, P.A., Hanchare, P.P., Manikshete, A.H., Sankpal, U.B. and Bhuse, V.M. (2016) Structural, Opto-Electronic and Photoelectrochemical Properties of Tungsten Diselenide Thin Films. *Applied Nanoscience*, **6**, 191-196. https://doi.org/10.1007/s13204-014-0388-0

[13] Patterson, A.L. (1939) The Scherrer Formula for X-Ray Particle Size Determination. *Physical Review,* **15**, 978-985. https://doi.org/10.1103/PhysRev.56.978

[14] Denton, A.R. and Ashcroft, N.W. (1991) Vergard's Law. *Physical Review A* (*Atomic*, *Molecular*, *and Optical Physics*), **43**, 3161-3164. https://doi.org/10.1103/PhysRevA.43.3161